Spectroscopy of Hydrothermal Reactions 15. The pH and Counterion Effects on the Decarboxylation Kinetics of the Malonate System

N. R. Gunawardena and T. B. Brill*

Department of Chemistry and Biochemistry, University of Delaware, Newark, Delaware 19716

Received: October 4, 2000

Malonic acid ($HO_2CCH_2CO_2H$) and its anions malonate(−1) ($HO_2CCH_2CO_2^-$) and malonate(−2) ($^-O_2CCH_2CO_2^-$) are among the more abundant dicarboxylates in natural water. Two variables influencing their behavior are the pH and the counterion. The rate constants for decarboxylation were determined in the pH range of 1.89−7.0 with a flow reactor−FTIR spectroscopy cell operating at 140−240 °C and 275 bar. The relative rates of the first-order reactions are malonic acid > malonate(−1) ≫ malonate(−2). The Arrhenius activation energies are similar for the three species (116−120 kJ/mol), making the rate differences controlled primarily by the pre-exponential factors ln(A, s^{-1}) = 30.2, 28.3, and 23.3, respectively]. These findings are interpreted in terms of the role of entropy in a cyclic intermediate common to all three species. Malonate(−2) is proposed to form this structure by hydration to 1-orthomalonate(−2). The entropy decreases as the negative charge increases due to increased rigidity of the cyclic intermediate and increased electrostriction of the solvation shell. The influence of the Group 1 and 2 cations Li^+, Na^+, K^+, Rb^+, Cs^+, Mg^{2+}, Ca^{2+}, and Sr^{2+} on the decarboxylation rate of malonate(−1) was determined. Except for Mg^{2+}, the rate decreases with increasing ionic potential (ion charge/ion radius), which is consistent with increasing replacement of H by the metal ion in the six-member cyclic intermediate. Mg^{2+} is anomalous possibly because it forms the strongest complex with malonate(−1) and decarboxylates by a different mechanism.

Introduction

The kinetics and mechanisms of reactions in water at high temperature and pressure (i.e., hydrothermal conditions) are important features of many geochemical and industiral processes.[1] Malonates are among the most important dicarboxylate compounds in the formation waters of oil fields in the crust of the Earth, but the speciation of malonate depends on the pH. The neutral acid structure I dominates at pH <1.9, the monoanion structure II [malonate(−1)] dominates at pH 4, and the dianion structure III [malonate(−2)] dominates at pH >7. The total concentration of malonate has been reported to be as high as 2540 ppm in natural water,[2] although values less than a few hundred parts per million are more commonly found.[3]

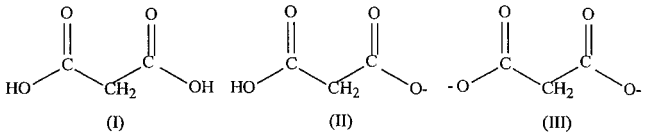

Because the concentrations of simple aliphatic carboxylic acids in natural hydrothermal water are partly controlled by their inertness toward the decarboxylation reaction 1, knowledge of the kinetics of decarboxylation at high temperatures and pressures is especially important[4]

$$RCH_2C(O)OH \rightarrow RCH_3 + CO_2 \qquad (1)$$

Such determinations can be difficult to interpret, however, if heterogeneous and homogeneous pathways compete in determining the observed rate of reaction 1. In an earlier study, we determined that the rates of decarboxylation of malonic acid and sodium malonate(−1) at hydrothermal conditions are relatively independent of the metal used to construct the cell.[5−7] Thus, the reaction can be considered to occur predominantly by the homogeneous pathway as opposed to being heterogeneously catalyzed.[4]

In addition to these recent hydrothermal studies, the decarboxylation kinetics have been reported for aqueous malonic acid and sodium malonate(−1) below 100 °C.[8−10] Hall[10] found that the observed rate constant k_{obs} in the pH range of 0.42−4.89 was a simple function of k_1 and k_2 according to eq 2, where k_1 and k_2 are the decarboxylation rate constants for malonic acid and sodium malonate(−1), respectively. The variable x determined the concentration of each species

$$k_{obs} = k_1(a - x) + k_2(x) \qquad (2)$$

Malonate(−1) decarboxylates more slowly than malonic acid, which has been interpreted to result from resonance stabilization of the anion.[7] The kinetics of decarboxylation of the malonate(−2) ion have not been determined previously, although the rate is known to be much slower than those of the other two forms.[9]

The rate of decarboxylation of the malonate system was determined herein at pH 4−7, where the malonate(−1) and malonate(−2) ions dominate. When combined with the prevoius data for malonic acid, this information provides additional insight into the rate controlling factors. The measurements were made in real-time in a flow reactor using FTIR spectroscopy[11,12] by detecting the rate of formation of CO_2. The kinetic behavior at pH >4 could not be modeled in the same manner as that used for pH 0.4−4.9, where an equation having the form of eq 2 applied.[10]

* Corresponding author. E-mail: brill@Udel.edu.

10.1021/jp003612e CCC: $20.00
Published on Web 02/10/2001

In addition to the pH dependence, the effect of different countercations on the homogeneous decarboxylation rate was determined because a variety of inorganic ions are usually present in natural waters. The O-atoms of the malonate ion are positioned to chelate a metal ion to form a six-member ring. Such complexation of Al^{3+} is thought to contribute to the secondary porosity of sandstone,[13] although this source of secondary porosity has been disputed.[14] Nonetheless, association of malonate with metal ions is potentially important in Earth processes.[15−17] To understand the role of the cation in determining the decarboxylation rate of malonate(−1), we studied solutions in which Li^+, Na^+, K^+, Rb^+, Cs^+, Mg^{2+}, Ca^{2+}, and Sr^{2+} were the counterions. The variety of metal ions suitable for this work was limited by the low solubility of the product carbonates of most di- and trivalent metal ions, which caused the flow cell to plug at hydrothermal conditions. In general, however, both the pH dependence and the counterion effect cast light on some of the factors that control the hydrothermal decarboxylation rate of the malonate species.

Experimental Section

Malonic acid (Aldrich Chemical Co., 99%) and MOH (M = Li, Na, K, Rb, Cs) or $M(OH)_2$ (M = Mg, Ca, Sr) were combined to make the malonate solutions by using the following procedure. Milli-Q water (18 Ω) was sparged with Ar to remove atmospheric gases. A 0.50 *m* (molality, in moles/kilogram of solvent), the malonic acid solution (pH 1.89) was titrated with the appropriate concentration of metal hydroxide solution until the equivalence point was reached while maintaining the total malonate concentration at 0.25 *m*. The stoichiometries used were M(malonate) for Group 1 cations and $M(malonate)_2$ for Group 2 cations. For the pH-dependent studies of the sodium malonate solutions, the pH values used were 4.0−5.5 in 0.5 increments and 7.0. Kinetic data at pH 8−10 were less reliable and therefore not reported because of the extensive hydrolysis of CO_2 to HCO_3^- and CO_3^{2-}. The pH values were measured at 22 °C by the use of an Orion 330 pH meter with an Ag/AgCl perpHect electrode.

The flow reactor and spectroscopy cell used for this work have been described previously in detail.[11,12] The cell body was constructed of grade 2 titanium drilled to accept cartridge heaters and thermocouples. Infrared spectral measurements in the transmission mode at hydrothermal conditions were accomplished by compressing a gold foil disk into which a slot had been cut, thus creating a path length of 20 μm between two sapphire windows. The slot enabled the fluid to enter the cell, pass by the windows as a thin sheet, and exit. The path length was constant throughout the measurements, although the interference fringes became increasingly intense as the pH increased. This effect was reversible, which suggests that the surface reflectivity of the sapphire windows is altered by the presence of excess OH^-. Visual examination of the cell components showed no sign of corrosion. A computer program written in Visual Basic and enabled the temperature, pressure, and flow rate to be set and continuously controlled as desired within ±1 °C, ±1 bar, and ±0.01 mL/min, respectively. Temperatures of 140−240 °C at 275 bar pressure were required for these studies and provided a single fluid phase of 0.84−0.94 gm/cm^3 density based on pure water. The flow rates used were 0.10−1.00 mL/min, which convert to residence times of 45−4.5 s using the internal volume of the cell of 0.0819 cm^3. A correction was made for the density change of water with temperature at constant pressure.

The decarboxylation reaction rate was measured in real time by following the intensely absorbing asymmetric stretching mode of CO_2 at 2343 cm^{-1} using a Nicolet Magna 560 FTIR spectrometer. Thirty-two scans were summed at 4 cm^{-1} resolution at each flow rate. After subtracting the water background at the same temperature and pressure, we fit the CO_2 absorption profile with a four-parameter Voigt function to obtain the area. The IR absorptivity of CO_2 at constant concentration depends on the temperature[18] so that a correction must be applied. The rate constants resulting from these time-dependent concentrations were the average of 4−6 independent measurements. The weighted least-squares statistical methods were used, and care was taken when converting to log space, as discussed previously.[19] Corrections discussed below were necessary to account for the hydrolysis of CO_2 as the solution was made more basic.

Results and Discussion

Effect of pH on the Decarboxylation Rate. The malonate system consists of two pH-dependent equilibrium reactions 3 and 4

$$HO(O)CCH_2C(O)OH \rightleftarrows HO(O)CCH_2C(O)O^- + H^+ \quad (3)$$

$$HO(O)CCH_2C(O)O^- \rightleftarrows {}^-O(O)CCH_2C(O)O^- + H^+ \quad (4)$$

As mentioned in the Introduction, Hall[10] found that the observed decarboxylation rate of the species in reaction 3 at pH 0.42−4.89 at 90 °C was the simple weighted sum of the rates of decarboxylation of malonic acid and the malonate(−1) ion (reactions 5 and 6). Also, as noted above, malonic acid is the sole species at pH <1.9, malonate(−1) is the sole species at pH 4, and malonate(−2) is the sole species at pH >7

$$HO(O)CCH_2C(O)OH \rightarrow CH_3C(O)OH + CO_2 \quad (5)$$

$$HO(O)CCH_2C(O)O^- \rightarrow CH_3C(O)O^- + CO_2 \quad (6)$$

$${}^-O(O)CCH_2C(O)O^- + H_2O \rightarrow CH_3C(O)O^- + OH^- + CO_2 \quad (7)$$

The acetic acid and acetate products of these reactions are stable with respect to decarboxylation until a much higher temperature is reached.[20]

In accordance with these facts, we previously modeled the rate of decarboxylation of a malonic acid solution at 120−240 °C and 275 bar with a rate expression constructed from the individual rates for malonic acid and the malonate(−1) ion by the use of real-time measurements of the CO_2 concentration.[5] Figure 1 shows the absorption of $m_3(CO_2)$ produced by 0.25 *m* sodium malonate(−1) at 160 °C and several residence times in the flow cell. In the present study, the pH dependence of these data, however, cannot be used directly to calculate the rates of decarboxylation because of the various equilibria that come into play. Instead, the procedure described below ensured that the rates were treated correctly.

The use of CO_2 to measure the pH dependence of decarboxylation of the malonate(−1) and malonate(−2) ions by reactions 6 and 7 is complicated by partial hydrolysis of CO_2 according to eq 8

$$H_2O + CO_2 \overset{K_{a1}}{\rightleftharpoons} HCO_3^- + H^+ \overset{K_{a2}}{\rightleftharpoons} CO_3^{2-} + 2H^+ \quad (8)$$

As a result, the total aqueous CO_2 concentration $[CO_2]_{tot}$ cannot be directly obtained from the observed area of the CO_2 absorbance at 2343 cm^{-1}. Instead, eq 9 must be considerd at

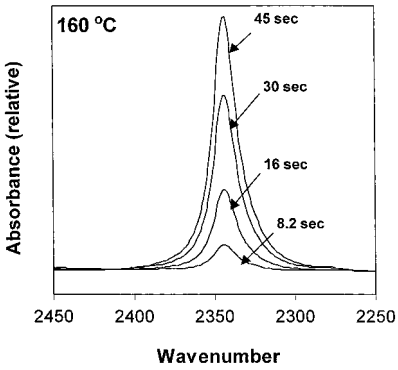

Figure 1. Illustration of $\upsilon_3(CO_2)$ from the decarboxylation of 0.25 *m* sodium malonate(−1) at 160 °C under 275 bar with several residence times in the flow reactor.

each temperature and pH value

$$[CO_2]_{tot} = [CO_2]_{obs} + [HCO_3^-] + [CO_3^{2-}] \quad (9)$$

Equilibrium reactions 3, 4, and 8 also contribute differently depending on the pH and temperature.

To determine all of the necessary equilibrium constants in water as a function of temperature, it is useful to rewrite the reactions in iso-Coulombic form,[21] such as 3 and 4 in terms of 10 and 11, to account for the change of K_w of water with temperature

$$HO(O)CCH_2C(O)O^- + H_2O \overset{K_1}{\rightleftharpoons} HO(O)CCH_2C(O)OH + OH^- \quad (10)$$

$$^-O(O)CCH_2C(O)O^- + H_2O \overset{K_2}{\rightleftharpoons} HO(O)CCH_2C(O)O^- + OH^- \quad (11)$$

As the decarboxylation reactions 5−7 take place, the acetate species formed also must be treated iso-Coulombically according to eq 12

$$CH_3C(O)O^- + H_2O \overset{K_3}{\rightleftharpoons} CH_3C(O)OH + OH \quad (12)$$

Thus, the values of the equilibrium constants K_1, K_2, and K_3 at the reaction temperature were determined by the iso-Coulombic extrapolation method from lower temperature literature values of dissociation constants of malonate and acetate species[22,23] and K_w.[24] Because the pH of the solution increases during the reaction, the carbonate species in eq 8 increasingly form. The values of K_{a1} and K_{a2} were obtained from literature[25] and were extrapolated to the desired temperature using the isoCoulombic method.

Since the ionic carbonate species do not absorb in the IR band-pass available, the kinetics of decarboxylation must be determined solely by the CO_2 asymmetric stretching mode at 2343 cm^{-1}, followed by conversion to $[CO_2]_{tot}$ via eq 9. $[CO_2]_{tot}$ also equals the initial concentration of the malonate species minus the concentration at time, *t*. Therefore the pH must be known at all times. The running concentration of OH^- can be determined by parametrizing the charge conservation eq 13 in terms of the equilibrium constants as shown in eq 14

$$[Na^+] + [H^+] = [OH^-] + [HOC(O)CH_2CO_2^-] + 2[^-OC(O)CH_2CO_2^-] + [CH_3CO_2^-] + [HCO_3^-] + 2[CO_3^{2-}] \quad (13)$$

$$\frac{K_w}{[OH^-]} = [OH^-] + \frac{A_{T(1)}K_2[OH^-]}{K_1K_2 + K_2[OH^-] + [OH^-]^2} + \frac{2A_{T(1)}[OH^-]^2}{K_1K_2 + K_2[OH^-] + [OH^-]^2} + \frac{A_{T(2)}[OH^-]}{K_3 + [OH^-]} + \frac{C_TK_wK_{a1}[OH^-]}{K_w^2 + K_wK_{a1}[OH^-] + K_{a1}K_{a2}[OH^-]^2} + \frac{2C_TK_{a1}K_{a2}[OH^-]^2}{K_w^2 + K_wK_{a1}[OH^-] + K_{a1}K_{a2}[OH^-]^2} \quad (14)$$

The total amount of malonate is $A_{T(1)}$ ($[HOC(O)OCH_2CO_2H] + [HOC(O)CH_2CO_2^-] + [^-OC(O)OCH_2CO_2^-]$). The total amount of acetate is $A_{T(2)}$ ($[CH_3CO_2H] + [CH_3CO_2^-]$). The total amount of carbonate C_T is eq 9. Differentiation of eq 14 yields eq 15, which provided $[OH^-]$ at any time during the reaction. The model shows that $[OH^-]$ increases slightly as the reaction progresses, i.e., at longer residence times. For example, the pH of sodium malonate(−1) at 190 °C is initially 4.16. This value rises to 4.50 at 18 s, at which time the reaction is about 50% complete

$$[d[OH^-]/dt] = [dA_{T(1)}/dt]\{(K_1K_2^2[OH^-] + K_2^2[OH^-]^2 + 3K_2[OH^-]^3 + 2K_1K_2[OH^-]^2 + 2[OH^-]^4)/(K_1K_2 + K_2[OH^-] + [OH^-]^2)^2] + [dC_T/dt][(K_{a1}K_w^3[OH^-] + K_{a1}^2K_w^2[OH^-]^2 + 3K_{a1}^2K_{a2}K_w[OH^-]^3 + 2K_w^2K_{a1}K_{a2}[OH^-]^2 + 2K_{a1}^2K_{a2}^2[OH^-]^4)/(K_w^2 + K_wK_{a1}[OH^-] + K_{a1}K_{a2}[OH^-]^2)^2] + [dA_{T(2)}/dt)([OH^-]/(K_3 + [OH^-])\}/\{[1 + K_w/[OH^-]^2 + (K_1K_2^2A_{T(1)} + K_2A_{T(1)}[OH^-]^2 + 4K_1K_2A_{T(1)}[OH^-])/(K_1K_2 + K_2[OH^-] + [OH^-]^2)^2 + (K_{a1}A_{T(2)} - [OH^-]A_{T(2)})(K_{a1} + [OH^-])^2] + [(K_w^3K_{a1}C_T + K_wK_{a1}^2K_{a2}C_T[OH^-]^2 + 4K_w^2K_{a1}K_{a2}C_T[OH^-])/(K_w^2 + K_wK_{a1}[OH^-] + K_{a1}K_{a2}[OH^-]^2)^2]\} \quad (15)$$

After $[CO_2]_{tot}$ is determined from $[CO_2]_{obs}$ using eqs 8 and 9, Figure 2 illustrates the first-order rate plots for reaction 6 at several temperatures. The rate constants for reactions 6 and 7 are given in Tables 1 and 2, respectively. It is more correct to refer to these rate constants as pseudo-first-order because the surrounding water field is hydrogen bonded to the malonate ion and cannot be excluded in the proton-transfer steps leading to the products (vide infra). The resulting Arrhenius plots for pH 4.0−5.5 are shown in Figure 3. Also included is the Arrhenius plot at pH 7.0, where malonate(−2) is the dominant species. It should be noted that curvature was observed in the Arrhenius plots at higher temperature (greater extent of reaction) when $[CO_2]_{obs}$ was used. The curvature resulted from the formation of soluble carbonates, which are not taken into account when $[CO_2]_{obs}$ alone is used. The plots were linear, however, when all of the carbonate species were included by using $[CO_2]_{tot}$. According to Figure 3, the rate clearly decreases

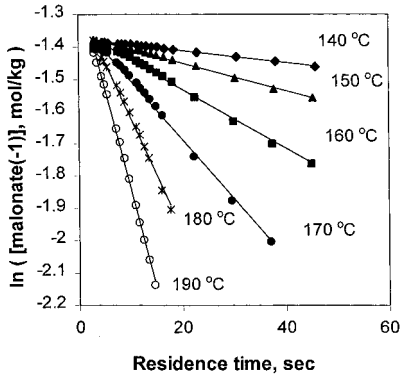

Figure 2. Pseudo-first-order rate plots for 0.25 *m* sodium malonate(−1) at 275 bar.

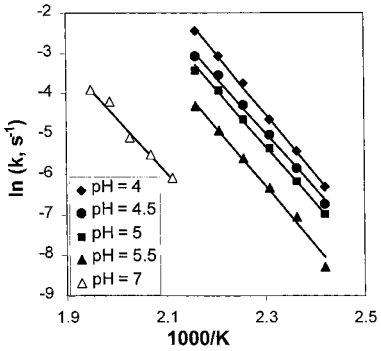

Figure 3. Arrhenius plots for the decarboxylation of sodium malonate(−1) at pH 4−5.5 and sodium malonate(−2) at pH 7.

TABLE 1: Pseudo- First-Order Rate Constants for Decarboxylation of Sodium Malonate(−1) at pH 4 − 5.5 under 275 bar

	k ($s^{-1} \times 10^3$)			
T (°C)	pH 4	pH 4.5	pH 5	pH 5.5
140	1.82 ± 0.32	1.18 ± 0.37	0.92 ± 0.02	0.25 ± 0.12
150	4.39 ± 0.73	2.86 ± 0.72	2.08 ± 0.51	0.86 ± 0.40
160	9.69 ± 1.4	6.63 ± 1.61	4.68 ± 1.19	1.78 ± 0.71
170	23.6 ± 11.8	13.69 ± 3.23	9.62 ± 1.94	3.67 ± 1.36
180	46.4 ± 18.1	29.07 ± 6.93	19.89 ± 2.94	7.46 ± 2.93
190	87.18 ± 38.0	46.70 ± 6.01	32.56 ± 6.61	13.41 ± 4.33

TABLE 2: Pseudo-First-Order Rate Constants for the Decarboxylation of Sodium Malonate(−2) at pH 7 under 275 bar

T (°C)	*k* ($s^{-1} \times 10^3$)
200	2.24 ± 0.41
210	4.02 ± 0.83
220	6.19 ± 1.16
230	15.05 ± 5.02
240	20.3 ± 1.61

with increasing pH in the range of 4−5.5. This result is at odds with that of Hall,[10] where the rate was independent of the pH in the 4−4.89 range. Unlike Hall's finding for the pH range of 0.4−4.89, an equation having the form of eq 2, but using the malonate(−1) and malonate(−2) rates, failed to model the rates obtained in the pH 4.0−5.5 range. Instead, the observed rate was controlled entirely by the malonate(−1) concentration, which was calculated from the equilibrium constant for eq 4[22,23] at the reaction temperature using the isoCoulombic method. This is demonstrated in Figure 4, which is a plot of the molality of malonate(−1) versus the rate constants at each pH value at 160 °C. In summary, eq 2 can be applied at pH <4 at 120−190 °C because the decarboxylation rates of both malonic acid and sodium malonate(−1) are sufficiently similar to contribute at

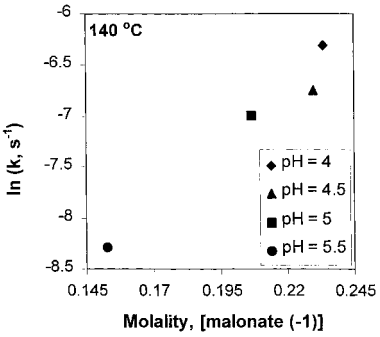

Figure 4. Plot of the calculated molality of sodium malonate(−1) at 140 °C and various values of the pH vs the rate constant for decarboxylation. The correlation suggests that the pH effect is the result of different concentrations of malonate(−1).

TABLE 3: Arrhenius Parameters for the Decarboxylation of Malonic Acid, Malonate (−1), and Malonate (−2) Salt under 275 bar

compound	E_a (kJ/mol)	ln *A* (s^{-1})	$\Delta S^{\ddagger}$ (J/mol K)
malonic acid	120.0 ± 1.3	30.2 ± 1.1	−6.1
sodium malonate(−1)	118.0 ± 8.0	28.3 ± 1.2	−21.5
sodium malonate(−2)	116.0 ± 2.1	23.3 ± 1.2	−63.4

these conditions. At pH 4−5.5 in this temperature range, the observed decarboxylation rate is controlled solely by malonate(−1) concentration. The rate for malonate(−2) only contributes above 200 °C.

The Arrhenius plot shown in Figure 5 compares the decarboxylation kinetics of 0.25 *m* solutions of malonic acid, malonate(−1), and malonate(−2). The Arrhenius parameters are given in Table 3. It is noteworthy that the activation energies E_a are nearly the same for the three forms of malonate (116−120 kJ/mol) and the preexponential factors are mainly responsible for the difference in the observed rates. The similarity of the E_a values suggests that a similar transition state for decarboxylation may exist for all three species. It has been suggested in past work[4,5,7,26−29] that the rates for malonic acid and malonate(−1) are enhanced by the existence of the cyclic structure IV and that this intermediate facilitates internal H-atom transfer with elimination of CO_2 according to reaction 16. The fact, however, that malonate(−2) has essentially the same activation energy as the others but cannot form structure IV directly suggests that it is necessary to hydrate one of the carboxylate groups and form the "orthomalonate" ion by reaction 17.

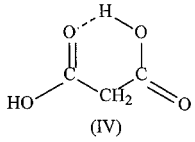

(IV)

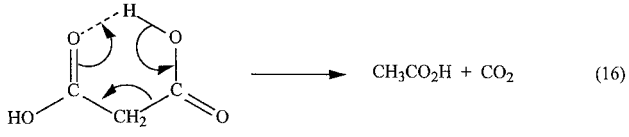

(16)

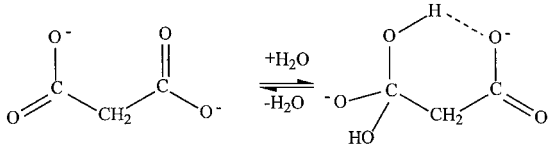

(17)

Reaction 17 is known to occur with a variety of carboxylic acids in basic solution.[30] Thus, an intermediate resembling IV can exist with the three forms of malonate.

TABLE 4: Pseudo-First-Order Rate Constants for the Decarboxylation of Group 1 and 2 Malonate(−1) Salts under 275 bar

	k ($s^{-1} \times 10^3$)					
	$T = 140$ °C	$T = 150$ °C	$T = 160$ °C	$T = 170$ °C	$T = 180$ °C	$T = 190$ °C
Li	1.75 ± 0.42	4.26 ± 0.81	9.26 ± 1.83	18.25 ± 2.78	34.45 ± 4.48	61.94 ± 5.17
Na	1.87 ± 0.34	4.52 ± 0.79	10.03 ± 1.54	19.98 ± 2.94	41.28 ± 5.07	93.86 ± 45.2
K	1.90 ± 0.33	4.61 ± 0.78	10.15 ± 1.73	20.67 ± 2.48	41.69 ± 3.04	74.41±6.72
Rb	2.49 ± 0.17	5.88 ± 0.38	12.94 ± 0.79	26.59 ± 3.06	51.27 ± 5.24	96.36 ± 21.4
Cs	2.41 ± 0.21	5.70 ± 0.61	12.36 ± 1.43	24.80 ± 2.95	48.16 ± 7.88	95.29 ± 11.6
Mg	1.62 ± 0.05	4.10 ± 0.30	8.75 ± 0.57	15.86 ± 1.91	30.98 ± 4.25	
Ca	0.99 ± 0.05	2.40 ± 0.098	5.43 ± 0.18	11.31 ± 0.50	21.83 ± 0.86	
Sr	1.40	3.28				

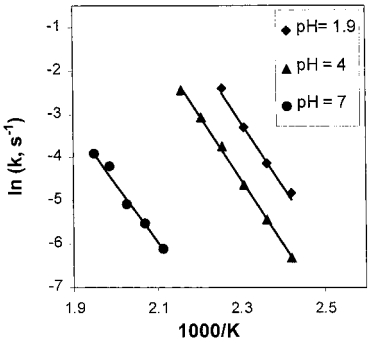

Figure 5. Arrhenius plots for the decarboxylation of malonic acid (pH 1.9), sodium malonate(−1) (pH 4.0), and sodium malonate(−2) (pH 7.0).

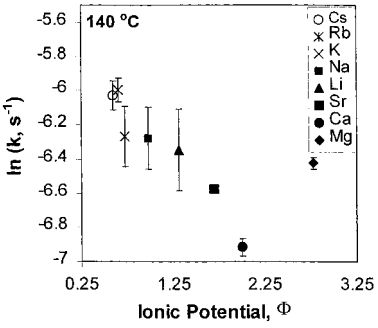

Figure 6. Effect of the counterion on the decarboxylation rate in 0.25 *m* solutions of malonate(−1) at 140 °C and 275 bar.

The pre-exponential *A* factor, which differs with the form of malonate (Table 3), is a reflection of the entropy of activation of the decarboxylation process. The magnitude and sign of $\Delta S^{\ddagger}$ are consistent with the existence of an associative transition state. The mechanism proposed above implies an entropy loss in the order malonate(−2) > malonate(−1) > malonic acid. This trend is consistent with the fact that (i) the cyclic intermediate (and thus the transition state) becomes increasingly rigid as the negative charge increases and (ii) the H_2O molecules in the solvation shell are expected to be increasingly electrostricted. Both of these factors disfavor the decarboxylation reaction by the mechanism proposed because they reduce the entropy of the system. It should be noted that nucleophilic attack at the carbonyl carbon position by amine bases has been suggested to contribute to the decarboxylation of malonic acid.[27,28] Nucleophilic attack by H_2O at this position possibly contributes in the case of malonic acid but is less likely in the malonate(−1) and malonate(−2) forms because the carbonyl carbon atom loses its electrophilicity.

The Effect of the Countercation on the Decarboxylation Rate. Natural waters contain a variety of cations, both main group and transition metal, that might associate with the malonate ions. In principle, the malonate ion is well suited to incorporate metal cations into the six-member ring equivalent of structure IV. The stability constants (p*K*) of complexes between oxygen donor anions and Group 1 cations, however, indicate that in some cases less than 10% ions are complexed at 25 °C.[31] For example, p$K = -0.18$ for sodium acetate. The p*K* values for the citrate salts of Cs^+ and Li^+ are 0.32 and 0.83, respectively. The only p*K* data available for the malonate (−1) salts are for Na^+ (0.74), Mg^{2+} (2.15), Ca^{2+} (1.57 and 2.9 ± 0.3 at 90 °C[17]), and Sr^{2+} (1.30).[31]

The alteration of the decarboxylation rate of malonate(−1) caused by different concentrations of the countercations has been investigated in the 55−90 °C range for Al^{3+}, Ga^{3+}, Ni^{2+}, Zn^{2+}, and Ca^{2+}.[32] Complexation was found to retard the decarboxylation rate compared to malonic acid. Owing to complications mostly related to precipitation of metal carbonate and possibly oxide products that plugged the flow reactor, we were limited in our work to a study of the effect of the Group 1 and 2 elements on malonate(−1). Because of relatively weak complexation, the observed effect was frequently near the limit of error despite the use of real-time detection of the intensely IR-absorbing asymmetric stretching mode of CO_2. Group 1 cations Li^+, Na^+, K^+, Rb^+, Cs^+ and Group 2 cations Mg^{2+}, Ca^{2+}, and Sr^{2+} in stoichiometric 0.25 *m* malonate(−1) salt solutions were successfully characterized at 140−190 °C and 275 bar, although the low solubility of $SrCO_3$ limited the Sr^{2+} determination to 140 and 150 °C. Table 4 shows that despite the small differences in the rate constants for the Group 1 cations, the trend is the same at each temperature in the 140−190 °C range.[33] Figure 6 shows the rate constants at 140 °C plotted versus the ionic potential (ion charge/ion radius) of each cation. Except for Mg^{2+}, which will be discussed separately below, the trend is a decrease in the decarboxylation rate, with an increase in the ionic potential of the cation. This trend is consistent with that found by Fein et al. for other ions.[32] We believe that an explanation for this trend lies in the apparent role of structure IV in the decarboxylation process. The complexing power of these cations scales with the ionic potential. Metal ions, which more effectively compete with H for a position in the ring, would be expected to retard the reaction rate because internal H-atom transfer is eliminated.

Figure 6 shows that aqueous $Mg(O_2CH_2CO_2H)_2$ fails to follow the same pattern as that of the other cations studied. Three possible explanations were considered. First, Mg^{2+} has about the same ionic radius as that of Li^+ (71 vs.73 pm). The rates in Table 4 reveal that the decarboxylation rate resembles that of Li^+. If the ion were actually $MgOH^+$, the effective ionic potential would be less, which might lead to similar decarboxylation rates for Mg^{2+} and Li^+. At the pH value of the solution (3.64 at 30 °C), however, only a very small concentration of $MgOH^+$ is present. A second possible explanation is that the hydration sphere of the Mg^{2+} is tighter than the those of other ions such that it is less effectively complexed by the malonate ion. Hence, Mg^{2+} might produce decarboxylation of the malonate(−1) ion at a rate that is similar to those produced by the Group 1 ions. On the contrary, the hydration sphere of Mg^{2+}

is not unusual compared to those of other ions.[34] A third possible reason is the stronger complexation of malonate(−1) by Mg^{2+}, according to the stability constants given above. If decarboxylation occurs primarily from this complex, then the rate is expected to be greater because the negative charge on the malonate(−1) ion is somewhat neutralized. In this case, the electrophilicity of the carbonyl carbon atom is greater, which makes it more susceptible to nucleophilic attack by H_2O. Of the three rationalizations offered here, this latter one seems to be the most plausible.

Conclusions

The decarboxylation rates of malonate species as a function of pH at hydrothermal conditions appear to be controlled mainly by two factors. The first is the entropy loss in the cyclic intermediate due to greater rigidity brought on by the greater negative charge on the anion. The higher negative charge also decreases the total entropy by organizing the surrounding water molecules. The decarboxylation rates of the malonate(−1) salts of Group 1 and 2 counterions is mainly the result of the competition of the metal ions with H for a position in the six-member ring. The data show that weakly complexing cations tend to stabilize malonate up to a point primarily because of this effect. Limited experience with one more strongly complexing cation (Mg^{2+}) indicates that malonate can become slightly destabilized toward decarboxylation compared to weaky complexing ions. This is perhaps because the electrophilicity of the carbonyl carbon atom is enhanced, which makes this center more susceptible to nucleophilic attack by water.

Acknowledgment. We are grateful to the National Science Foundation for support of this work on Grant CHE-9807370. The comments of Dr. Robert Bach regarding the mechanism of decarboxylation were very helpful.

References and Notes

(1) Brill. T. B. *J. Phys. Chem. A* **2000**, *104*, 4343.
(2) MacGowan, D. B.; Surdam, R. C. *Org. Geochem*. **1988**, *12*, 245.
(3) Lundegard, P. D.; Kharaka, Y. K. In *Organic Acids in Geological Processes*; Pittman, E. D., Lewan, M. D., Eds.; Springer-Verlag: New York, 1993; Chapter 3.
(4) Bell, J. L. S.; Palmer, D. A. In *Organic Acids in Geological Processes*; Pittman, E. D., Lewan, M. D., Eds.; Springer-Verlag: New York, 1993; Chapter 9.
(5) Maiella, P. G.; Brill, T. B. *J. Phys. Chem.* **1996**, *100*, 14352.
(6) Maiella, P. G.; Brill, T. B. *J. Phys. Chem. A* **1998**, *102*, 5886.
(7) Belsky, A. J.; Maiella, P. G.; Brill, T. B. *J. Phys. Chem. A* **1999**, *103*, 4253.
(8) Bernoulli, A. L.; Wege, W. *Helv. Chim. Acta* **1919**, *2*, 613.
(9) Fairclough, R. A. *J. Chem. Soc*. **1938**, 1186.
(10) Hall, G. A. Jr. *J. Am. Chem. Soc*. **1949**, *71*, 2691.
(11) Kieke, M. L.; Schoppelrei, J. W.; Brill, T. B. *J. Phys. Chem*. **1996**, *100*, 7455.
(12) Schoppelrei, J. W.; Kieke, M. L.; Wang, X.; Klein, M. T.; Brill, T. B. *J. Phys. Chem.* **1996**, *100*, 14343.
(13) Surdam, R. C.; Boese, S. W.; Crosey, L. J. *Am. Assoc. Petrol. Geol. Mem*. **1984**, *37*, 127.
(14) Giles, M. R.; de Boer, R. B.; Marshall, J. D. In *Organic Acids in Geological Processes*; Pittman, E. D., Lewan, M. D., Eds.; Springer-Verlag: New York, 1993; Chapter 14
(15) Shock, E. L.; Koretsky, C. M. *Geochim. Cosmochim. Acta* **1993**, *57*, 4899; **1995**, *59*, 1497.
(16) Prapaipong, P.; Shock, E. L.; Koretsky, C. M. *Geochim. Cosmochim. Acta* **1999**, *63*, 2547.
(17) Fein, J. B.; Yane, L.; Jyoti, A.; Handa, T. *Geochim. Cosmochim. Acta* **1995**, *59*, 1053.
(18) Maiella, P. G.; Brill, T. B. *Appl. Spectrosc*. **1999**, *53*, 351.
(19) Cvetanovic, R. J.; Singleton, D. L. *Int. J. Chem. Kinet*. **1977**, *9*, 481.
(20) Meyer, J. C.; Marrone, P. A.; Tester, J. W. *AIChE J*. **1995**, *41*, 2108.
(21) Lindsay, W. T. *Proc. Int. Water Conf., Eng. Soc. West. Pa*. **1980**, *41*, 284.
(22) Kortüm, G.; Vogel, W.; and Andrussow, K. *Dissociation Constants of Organic Acids in Aqueous Solution*; Butterworths: Markham, Canada, 1961.
(23) Kettler, R. M.; Wesolowski, D. J.; and Palmer, D. A. *J. Solution Chem*. **1992**, *21*, 883.
(24) Marshall, W. L.; Franck, E. U. *J. Phys. Chem. Ref. Data* **1981**, *10*, 295.
(25) Butler, J. N. *Carbon Dioxide Equilibria and Their Applications*; Addison-Wesley: Reading, MA, 1991**.**
(26) King, J. A. *J. Am. Chem. Soc*. **1947**, *69*, 2738.
(27) Fraenkel, G.; Belford, R. L.; Yankwich, P. E. *J. Am. Chem. Soc*. **1954**, *76*, 15.
(28) Clark, L. W. In *The Chemistry of Carboxylic Acids and Esters. The Chemistry of Functional Groups Series*; Patai, S. Ed.; Wiley: New York, 1967; p 589.
(29) Bach, R. D.; Canepa, C. *J. Org. Chem*. **1996,** *61*, 6345.
(30) Shapiro, Y. M. Russian Patent SU 1836317, August 30, 1993.
(31) Martell, A. E.; Smith, R. M. *Critical Stability Constants*; Plenum Press: New York, 1977; Vol. 3.
(32) Fein, J. B.; Gore, N.; Marshall, D.; Yassa, L.; Loch, A.; Brantley, S. *Geochim. Cosmochim. Acta* **1995**, *59*, 5071.
(33) Brill, T. B.; Gunawardena, N. R.; Miksa, D. *High Pressure Res*., in press.
(34) Bulmer, J. T.; Irish, D. E.; Odberg, L. *Can. J. Chem.* **1975**, *53*, 3806.